Korean J. Chem. Eng., 36(8), 1328-1338 (2019)
DOI: 10.1007/s11814-019-0322-y

pISSN: 0256-1115
eISSN: 1975-7220

Competition of mixed divalent ions through supported liquid membranes: Co-ion and concentration effects on permeability

Thi Tuong Van Tran*,, Chiao-Chen Hsu*, Selvaraj Rajesh Kumar*, and Shingjiang Jessie Lue*,***,****,*****,†**

*Department of Chemical and Materials Engineering and Green Technology Research Center, Chang Gung University, Guishan District, Taoyuan 333, Taiwan
**Institute of Environmental Science, Engineering and Management, Industrial University of Ho Chi Minh City, Go Vap District, Ho Chi Minh City, Vietnam
***Department of Radiation Oncology, Chang Gung Memorial Hospital, Guishan District, Taoyuan 333, Taiwan
****Department of Safety, Health and Environmental Engineering, Ming-Chi University of Technology, Taishan District, New Taipei City 243, Taiwan
*****R&D Center for Membrane Technology, Chung Yuan Christian University, Chung Li District, Taoyuan 320, Taiwan
(*Received 14 February 2019 • accepted 1 June 2019*)

Abstract−Zn^{2+}, Cu^{2+} and Ni^{2+} permeabilities through supported liquid membranes (SLMs) were determined experimentally from single, binary, and ternary ionic mixtures. Microporous polypropylene membrane was used as the frame to retain isopar-L solvent and di (2-ethylhexyl) phosphoric acid (D2EHPA) carrier. Sulfuric acid solution was used as a strip (receiving) solution. The ion permeability values were in the 10^{-7}-10^{-6} cm^2 s^{-1} range and increased with the concentrations of D2EHPA in isopar-L and the stripping sulfuric acid. The ion ideal selectivity ranged from 1.05 (Zn/Cu) to 8.40 (Zn/Ni), depending on the feed concentration. The single ion permeability was significantly higher than the binary mixtures, probably due to ion competition with D2EHPA carrier molecules. High selectivity was achieved using ternary mixtures: Zn^{2+} was the fast-permeating species due to preferential sorption with D2EHPA. Separating Zn^{2+} from Cu^{2+} and/or Ni^{2+} mixtures was most efficient with high D2EHPA concentration, concentrated H_2SO_4 strip solution, concentrated feed solution, and from multiple ionic mixes.

Keywords: Zinc Separation and Recovery, Mobile Carrier, Separation Selectivity, Ionic Permeability, Ion Competition

INTRODUCTION

Heavy metals are elements with high atomic masses ranging between 63.5 u and 200.6 u, with specific gravities greater than 5.0 [1]. Most heavy metals are well-known to be toxic and carcinogenic. Heavy metals released into wastewater pose a serious threat to human health and the biodiversity of the receiving water bodies [1]. As one of the most dangerous environmental contaminants, heavy metals are faced with increasingly more stringent regulations from world governments. To protect water bodies and soils from being polluted by discharged heavy metals, the Environmental Protection Administration (EPA) in Taiwan and many countries began controlling heavy metal sources in accordance with the total quantity control program (TQC). Currently, the pollutants that are subject to TQC include copper (Cu), zinc (Zn), nickel (Ni), cadmium (Cd), chromium (Cr), and their ionic forms, which are present in the effluent generated through industrial processes such as plating, chemical engineering, dyeing and paper manufacturing [2,3].

In recent years, various conventional methods, including chemical precipitation [4], coagulation-flocculation [5], flotation [6], ion exchange [7,8], membrane filtration [9-12], adsorption [13-15] and extraction [16], have been proposed for the removal and recovery of heavy metals from aqueous solutions. Each of these techniques has its own intrinsic obstacles, such as sludge generation, extra operational cost for sludge disposal, high capital and operational cost, or susceptibility to fouling and inefficiency [17]. Consequently, novel, efficient and cost-effective methods for heavy metals separation have been continuously sought.

Among these techniques, liquid membrane, particularly supported liquid membrane (SLM), is a promising alternative to resolve the drawbacks of the conventional processes. The SLM process has pronounced advantages, such as combining extraction and stripping into a single stage (Fig. 1), and non-equilibrium mass-transfer characteristics [18]. Additionally, limitations like aqueous/organic phase ratio, emulsification, flooding and loading limits, phase disengagement, large solvent inventory, and so forth, can be avoided [19,20]. The stability period of SLMs may last several days [21,22], weeks [23,24] or even months [25] in many systems. Duan et al. [22] reported nearly consistent transport percentages of copper and nickel for at least seven days of continuous operation by employing the SLM with (TRPO+M5640) carrier in kerosene. Van De Voorde et al. [23] performed an ageing test on the Celgard membrane impregnated with (LIX 860-I+Cyanex 302) carrier for Watt's bath effluent and found stable nickel flux over 650 h. Moreover, the SLMs stability can be improved by proper selection of membrane materials and operating conditions and/or reimpregnation of the

†To whom correspondence should be addressed.
E-mail: jessie@mail.cgu.edu.tw

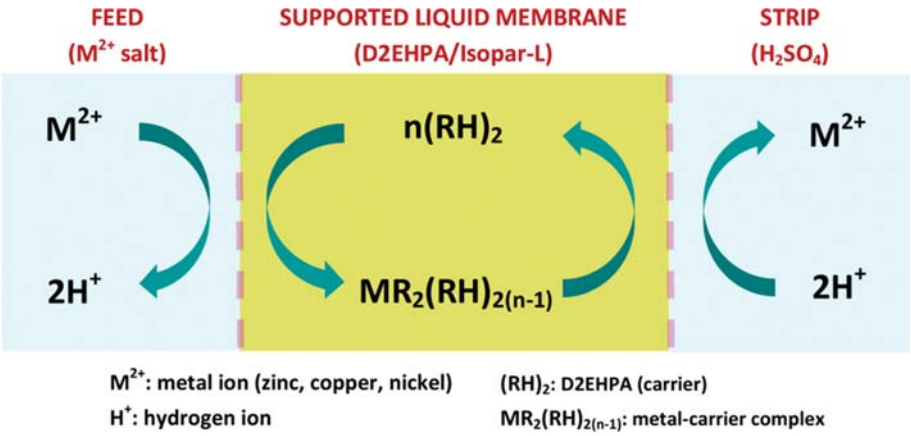

Fig. 1. Illustration of divalent cation transport through an SLM system. The metal ions in aqueous solution form complexes with carrier molecules, diffuse through the organic phase toward strip solution, and are released into sulfuric acid strip solution.

support, sandwich SLMs and gelation of SLMs [25]. To achieve high selectivity of an SLM, we can choose a special carrier in the organic liquid membrane for selectively removing one of the ions due to their preferential affinity.

The organic solvent, which is immiscible in the aqueous feed and strip solutions, preferably Isoparaffin Fluid (isopar-L) for its high stability and nonreactivity [26-28], is embedded in the microporous support to form an SLM. The carriers are usually surfactant-like molecules that form complexes with metal ions. One such carrier, di-(2-ethylhexyl) phosphoric acid (D2EHPA), a derivative of orthophosphoric acid, is widely utilized for metal extraction [29,30].

D2EHPA forms large complexes with metallic ions via cation-exchange mechanism near the aqueous feed-organic phase interface (as shown in the left part of Fig. 1). The carrier hydrophobic groups help the complexes to diffuse from the feed into the strip side (center part, Fig. 1). At the strip interface, the complexes undergo cation-exchange again and the metal ions are released into the strip solution. The carrier-metal complexes are dissociated and the metal-bonded carriers are exchanged with proton ions from the trip solution (right part, Fig. 1). Thus, the carriers are "regenerated" into the acidic form and able to continue complex formation.

Previous studies on applying the SLM technique for heavy metals removal and recovery have focused mainly upon the single ionic solution [23,31-36]. While, most industrial wastewaters contain more than one heavy metal, such as effluents from electroplating plants [37] and leaching liquors from spent mobile phone batteries [38]. It is therefore necessary to examine the simultaneous transport behavior of metal ions as well as to determine the interference by the presence of other ions on the permeability of the ion of interest in a multi-ionic mixture.

The overall aim of this paper was to carry out a comprehensive enquiry into the transport of a multi-ionic mixture of heavy metals through SLMs. We dealt with a tri-metal group comprised of Zn^{2+}, Cu^{2+} and Ni^{2+} because these elements are representative heavy metals of particular concern in industrial wastewater treatment [39]. Important operating parameters were investigated, including the carrier (D2EHPA) concentrations and the concentration of the feed and strip solutions. Furthermore, the effects of co-ions from binary and ternary ionic mixtures on the permeability were explored. The competitive mass transport behavior through the SLM was also elucidated.

EXPERIMENTAL

1. Materials and Methods

Polypropylene (PP) porous membranes were obtained from Celgard, LLC (2500, Charlotte, NC, USA) with a nominal porosity of 55%. Owing to high porosity, PP membranes can incorporate significant amounts of metal ion extractant and therefore are commonly employed as a membrane support in SLMs [40,41]. $ZnSO_4 \cdot 7H_2O$ was purchased from Scharlau (Barcelona, Spain), $CuSO_4 \cdot 5H_2O$ was purchased from YakuriPure Chemicals Inc. (Osaka, Japan), and $NiSO_4 \cdot 6H_2O$ was purchased from Showa Chemicals Inc. (Tokyo, Japan). The aqueous feed solution contained Zn^{2+}, Cu^{2+} and/or Ni^{2+} metal ions with concentrations ranging from ca 0.2 mM to 20 mM (10 ppm to 1,000 ppm) and pH of 2. The stripping solution was 0.9 or 1.8 M H_2SO_4, which was diluted from concentrated H_2SO_4 (from Showa Chemicals Inc.). D2EHPA was purchased from Merck (Kenilworth, NJ, USA). Organic solvent isopar-L (99%) was obtained from Exxon Mobile, Singapore, and acetone from Sigma-Aldrich (St. Louis, MO, USA). All solutions were freshly prepared with deionized (D.I.) water. All reagents were used without further purification.

2. Liquid Membrane Preparation

The liquid membrane was prepared using slightly modified procedures from the literature [42-44]. The PP support was cut into a circular disc with a diameter of 5 cm. After cleaning with acetone, the PP film was placed in a Buchner funnel and 250 mL of isopar-L containing various amounts (0-0.4 M) of D2EHPA was filtered through the PP film by applying suction from an aspirator. After this filtration process was repeated five times, the PP film was immersed in the isopar-L solution of corresponding D2EHPA concentration and ultrasonicated for 30 min to ensure the pores in the PP were fully filled with the isopar-L solution. The SLM-impregnated PP film was removed from the isopar-L solution and the surface was gently wiped with tissue paper to remove excess solution. This cleaning step was done carefully to ensure that no solution was lost from the membrane pores. A schematic diagram of the

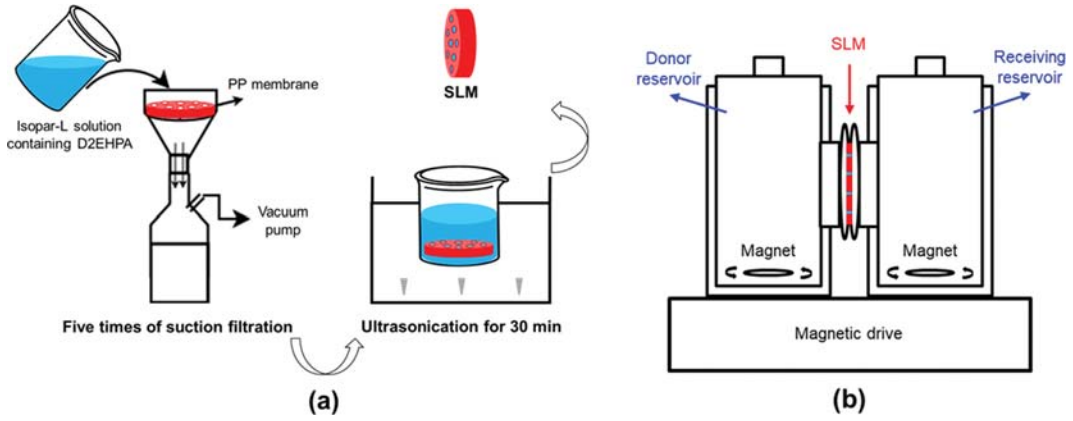

Fig. 2. Schematic representation of (a) SLM preparation, and (b) experimental setup for ion permeability measurement.

SLM preparation is depicted in Fig. 2(a).

3. Membrane Characterization

The PP film and that impregnated with SLM were examined using Fourier transform infrared spectroscopy (FTIR, Tensor-27, Bruker Corp., Billerica, MA, USA) to determine the chemical structure. The morphology and pore size distribution were analyzed using scanning electron microscopy (SEM, JSM-7500F, Japan Electron Optics Laboratory Co., Ltd., Tokyo, Japan) and capillary flow porometer (CFP, model 1500 AE, Porous Materials Inc., Ithaca, NY, USA).

4. Ion Permeability Measurement

The ion permeability was measured using a side-by-side diffusion permeation cell [45,46], which consists of two identical jacketed reservoirs with 25 mL capacity each, separated by the SLM (Fig. 2(b)). One reservoir (donor reservoir) was filled with salt feed solution and the other (receiving reservoir) with H_2SO_4 strip solution. Both the reservoirs were magnetically stirred at 300 rpm to prevent concentration polarization at the membrane interfaces and in the bulk of the solutions. The ion diffused from the donor to the receiving reservoir due to the concentration gradient. This process was conducted at 25±0.1 °C. A constant temperature was maintained to avoid any variations in the ion permeation rate which might be caused by changes in the aqueous and organic solution viscosities, carrier loss (related to its solubility in aqueous phases) and solvent evaporation [47,48]. Each experiment was performed for 2.5 h. Sampling was done by withdrawing 0.1 mL aliquots from the donor and receiving solutions at 0.5 h intervals to monitor the ion concentration. The ion concentration was determined using an inductively coupled plasma optical emission spectrometer (ICP-OES, 710-ES, Varian Inc., Palo Alto, CA, USA). The slope was calculated from the ion concentration in the receiving reservoir (strip solution) versus time plot. This linear regression coefficient, along with the 95% confidence interval, was determined and normalized to the initial feed concentration, strip solution volume, membrane area and membrane thickness to obtain the ion permeability (P, $cm^2\ s^{-1}$) [49]:

$$P = (\text{slope})\frac{\delta}{C_1}\frac{V}{A} \quad (1)$$

where δ is the membrane thickness (cm), V is the reservoir volume (cm^3), C_1 is the initial metal concentration (M) in the feed solution and A is the effective membrane area (cm^2).

To study the co-ion effect on the ion permeation rate, binary or ternary solutions containing $ZnSO_4$, $CuSO_4$, and/or $NiSO_4$ were mixed and used as feed solutions. Equal ionic concentration (0.2, 2, or 20 mM) was used for binary and ternary solutions to evaluate the feed concentration effect on the ion transport rate. The permeability ratios of any two of these ions can be used to calculate the separation selectivity (α) [50]:

$$\alpha = \frac{P_1}{P_2} \quad (2)$$

where P_1 and P_2 are the ion permeabilities of the two ions, respectively.

The concentrations of the as-prepared feed solutions and sampled aliquots from the strip solution were interpolated from the calibration curves (Fig. S1) established from standard solutions. Dilution could be made on these solutions so that the measured readings were within the calibration curve range.

RESULTS AND DISCUSSION

1. Membrane Characteristics

The chemical structure of the PP support and liquid membranes at different D2EHPA loads in isopar-L solvent were analyzed using FTIR, and the results are shown in Fig. 3(a). All the spectra reflect alkane structure of the PP support. The absorbance peaks at 2,850-3,000 cm^{-1}, 1,465 cm^{-1} and 1,450 cm^{-1} are due to alkanes stretching [51], -CH_2 bending and -CH_3 bending [52], respectively. These signal became stronger with the presence of isopar-L, also isoalkanes, in the liquid membranes compared with the PP support only. The spectra of D2EHPA liquid membranes exhibited new characteristic peaks of D2EHPA at 1,032 cm^{-1} and 1,232 cm^{-1}, which belong to -C-O-P- bending and P=O stretching, respectively [53-55]. These peaks show higher intensities at higher concentrations of D2EHPA. The FTIR interpretation confirms that D2EHPA was successfully incorporated into the liquid membranes at different amounts.

The PP support showed elongated pores in the sub-micron diameter range (Fig. 3(b)). ImageJ software was used to analyze several SEM images, and average pores were found as 0.291×0.028 μm, with an average porosity of 10%. The pore morphology was more

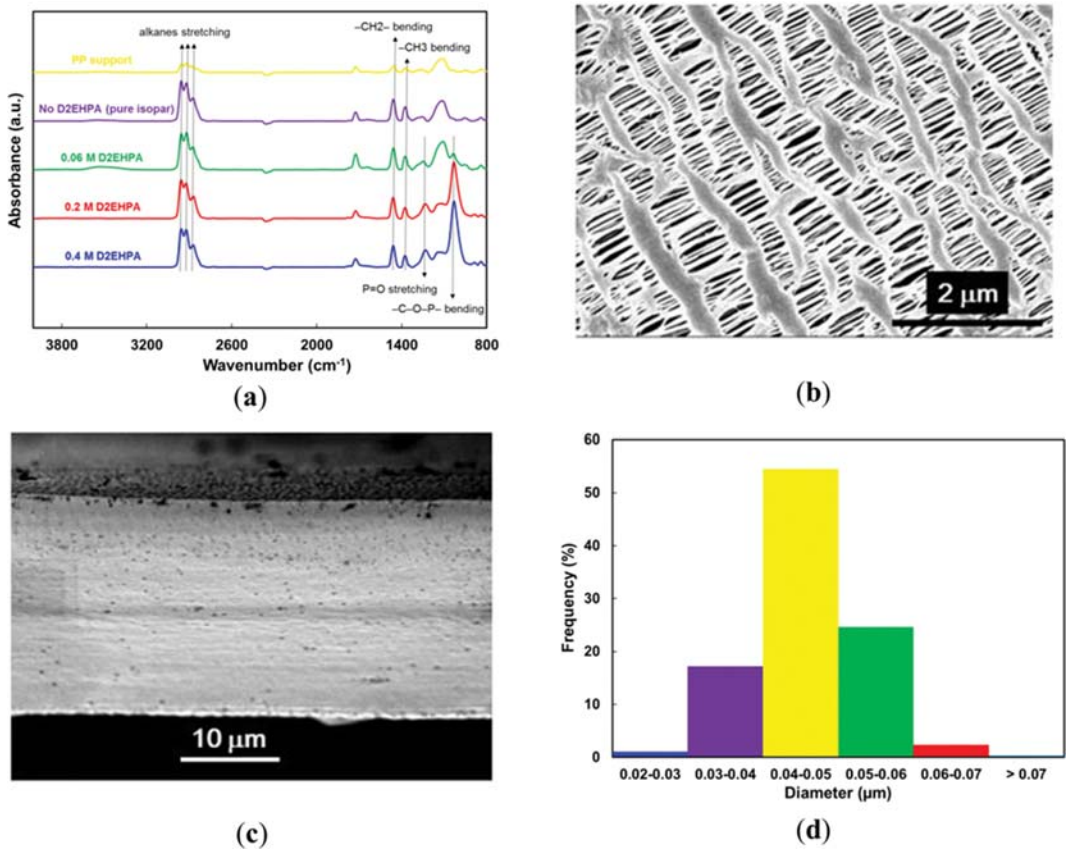

Fig. 3. (a) FTIR spectra of PP support and liquid membranes, (b) surface morphology, (c) cross-sectional image, and (d) hydraulic pore diameter distribution of porous PP support.

elongated than that reported in Surucu et al. [56]. The PP had uniform thickness of 24-25 μm (Fig. 3(c)). The hydraulic diameter distribution was analyzed using CFP and more than half of the pores were found to be in the 0.04-0.05 μm range, as shown in Fig. 3(d).

2. Effects of Carrier and Strip Solution Concentrations on Ion Permeability

In the first test the Zn^{2+} permeabilities were measured through the SLM as a function of the carrier (D2EHPA) concentration using 2 mM single salt solution as the donor solution and 0.9 M sulfuric acid aqueous solution as the receiving solution. The results are shown in Fig. 4. When pure isopar-L solvent (containing no D2EHPA) was used as the liquid membrane phase, the Zn^{2+} transported at a slow rate, with a permeated concentration of <0.02 mM in 2.5 h. The Zn^{2+} permeability was determined as $1.08\pm0.18\times10^{-8}$ cm^2 s^{-1}. As 0.06 M D2EHPA was added to the isopar-L solvent, this carrier formed a complex with Zn^{2+} [57], which could easily diffuse through the organic solvent (Fig. 1) and the permeation rate was increased. The Zn^{2+} permeability was raised to $7.88\pm0.81\times10^{-8}$ cm^2 s^{-1}, a seven-fold increase than that without D2EHPA. As the D2EHPA concentration was increased to 0.2 M, the Zn^{2+} permeability increased to $1.66\pm0.012\times10^{-7}$ cm^2 s^{-1}, a fifteen-fold increase from the control (pure isopar-L). These data confirmed the efficiency of D2EHPA in facilitating Zn^{2+} transfer through the organic solvent. A similar trend was also seen when Bhatluri et al. [58] varied carrier concentrations in the 0-0.5% (v/v) range during an SLM-based separation of cadmium from wastewater. It was reported that an increase in carrier concentration up to 0.5% (v/v) resulted in higher Cd^{2+} extraction and recovery. Since more carrier molecules react with metal ions at the feed-membrane interface, the rate of transportation increases.

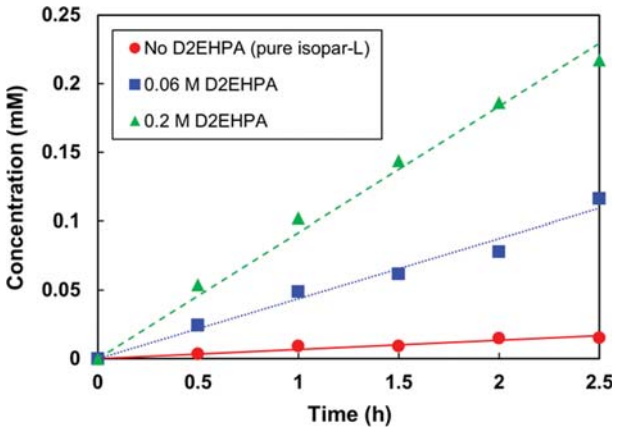

Fig. 4. Permeated Zn^{2+} concentration increase with time under low strip concentration and at different D2EHPA loads in isopar-L solvent. Donor phase: 2 mM Zn^{2+} ion; membrane: D2EHPA in isopar-L; receiving phase: 0.9 M H_2SO_4.

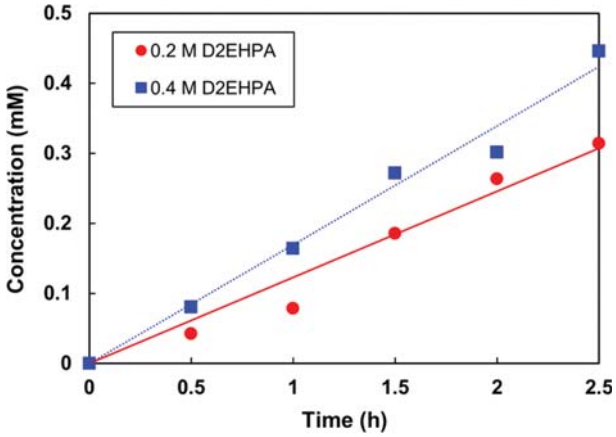

Fig. 5. Permeated Zn^{2+} concentration increase with time under high strip concentration and at different D2EHPA loads in isopar-L solvent. Donor phase: 2 mM Zn^{2+} ion; membrane: D2EHPA in isopar-L; receiving phase: 1.8 M H_2SO_4.

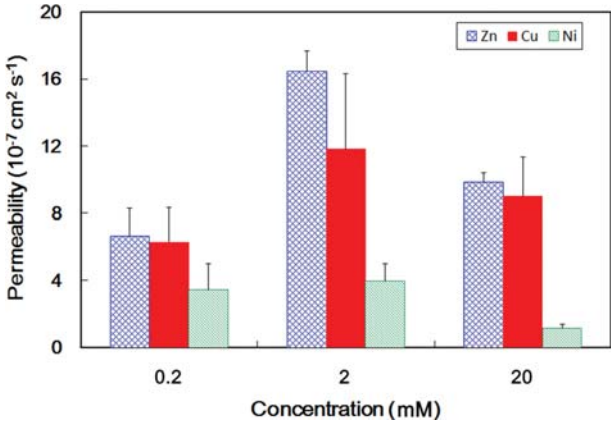

Fig. 7. Permeabilities of Zn^{2+}, Cu^{2+}, and Ni^{2+} from single solutions of various concentrations (with 1.8 M of initial H_2SO_4 concentration in strip solution and 0.4 M D2EHPA in isopar-L for membrane phase). Error bars indicate 95% confidence intervals.

The next test was to evaluate the effect of strip solution concentration. The H_2SO_4 concentration was increased from 0.9 M to 1.8 M and the results are presented in Fig. 5. When the D2EHPA concentration was maintained at 0.2 M, the Zn^{2+} permeability was determined as $2.78\pm0.30\times10^{-7}$ cm^2 s^{-1}, an increase by 67% from the lower H_2SO_4 concentration (0.9 M). The higher H_2SO_4 concentration helped the D2EHPA-Zn complex dissociate and exchange back to D2EHPA acid form [57] at the organic membrane and receiving phase interface (Fig. 1). The H_2SO_4 was then transformed into $ZnSO_4$; thus, the metal ions were transferred from the feed to the strip solution (Fig. 1). When the D2EHPA concentration was increased to 0.4 M, the Zn^{2+} permeability was further increased six-fold to $16.5\pm1.2\times10^{-7}$ cm^2 s^{-1}. In the following experiments, the D2EHPA concentration in the isopar-L was maintained at 0.4 M and the strip H_2SO_4 concentration was 1.8 M to enhance ion permeation rates.

3. Single Ion Permeability

The Zn^{2+}, Cu^{2+}, and Ni^{2+} permeabilities were measured through the SLM using 20 mM solution containing a single salt as the feed, 0.4 M D2EHPA in the membrane phase, and 1.8 M sulfuric acid aqueous solution as the receiving solution. The transport concentrations of Zn^{2+} ions through SLM increased linearly with time and increased to 2.19 mM at 2.5 h operation (as shown in Fig. 6). The same trend was observed for Cu^{2+} transport: permeated Cu^{2+} ion concentration linearly increased to 1.78 mM in 2.5 h (Fig. 6). The permeability values of Zn^{2+} and Cu^{2+} were similar: $9.83\pm0.57\times10^{-7}$ cm^2 s^{-1} and $9.01\pm2.33\times10^{-7}$ cm^2 s^{-1} for Zn^{2+} and Cu^{2+}, respectively (Fig. 7). On the other hand, the transport concentration of Ni^{2+} ions was only 0.18 mM after 2.5 h (Fig. 6), corresponding to a Ni^{2+} permeability of $1.17\pm0.20\times10^{-7}$ cm^2 s^{-1} (Fig. 7).

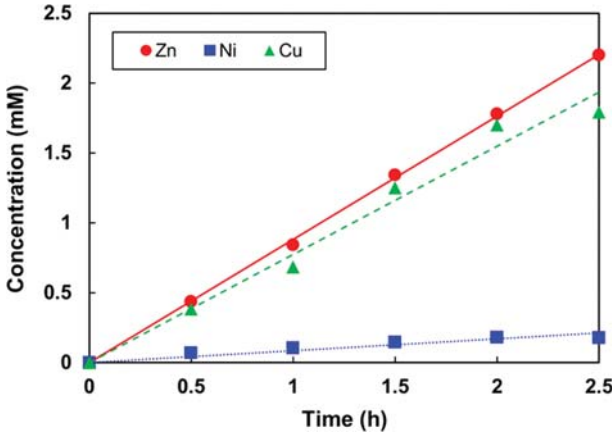

Fig. 6. Permeation of high-concentration (20 mM) of single Zn^{2+}, Cu^{2+}, and Ni^{2+} ions through SLM at various times (1.8 M of initial H_2SO_4 concentration in receiving solution and 0.4 M D2EHPA in isopar-L in membrane phase).

As the ion concentration was reduced to 2 mM, the Zn^{2+}, Cu^{2+}, and Ni^{2+} permeabilities were measured as $16.5\pm1.2\times10^{-7}$ cm^2 s^{-1}, $11.8\pm4.51\times10^{-7}$ cm^2 s^{-1} and $3.96\pm1.06\times10^{-7}$ cm^2 s^{-1}, respectively, as shown in Fig. 7. Further reducing the feed ion concentration to 0.2 mM, the Zn^{2+}, Cu^{2+}, and Ni^{2+} permeabilities were measured as $6.67\pm1.63\times10^{-7}$ cm^2 s^{-1}, $6.32\pm2.01\times10^{-7}$ cm^2 s^{-1}, $3.45\pm1.58\times10^{-7}$ cm^2 s^{-1}, respectively (Fig. 7).

The separation selectivity (α) indicates the relative permeability of any ion pairs. An α value close to unity means no separation efficiency using the SLM process, whereas a large or small value implies the ions can be separated due to differentiation of their transport rates. Here α values based on single solution (α_{single}) are used to represent the intrinsic properties of the ions without co-ion interference. The data are summarized in Table 1. It is clear that the α_{single} values of the Zn/Cu pair were almost 1.0 for 0.2-20 mM solutions, meaning the permeation rates between Zn^{2+} and Cu^{2+} were similar. At low concentration (0.2 mM), the α_{single} values for Cu/Ni and Zn/Ni pairs were 1.83 and 1.93, respectively. At medium concentration (2 mM), the α_{single} values for Cu/Ni and Zn/Ni pairs were increased to 2.98 and 4.16, respectively. At high concentration (20 mM), these values further increased to 7.70 and 8.41.

Zn^{2+}, Cu^{2+}, and Ni^{2+} have ion radii of 0.074 nm, 0.072 nm, 0.070 nm, and hydrated radii of 0.430 nm, 0.419 nm, 0.404 nm, respec-

Table 1. Selectivity (ratio of permeability for particular ion pair) from single, binary, and ternary solutions of 0.2, 2, and 20 mM

Concentration	0.2 mM		2 mM			20 mM		
	α_{single}	α_{binary}	α_{single}	α_{binary}	$\alpha_{ternary}$	α_{single}	α_{binary}	$\alpha_{ternary}$
Zn/Cu	1.05	1.98	1.39	1.25	10.2	1.09	2.87	21.2
Cu/Ni	1.83	1.22	2.98	4.63	0.37	7.70	2.80	1.27
Zn/Ni	1.93	1.37	4.16	3.46	3.81	8.41	58.2	27.0

tively [59]. Considering the diffusivity factor, the smaller ions may diffuse faster into the feed-membrane interface (Fig. 1). Accordingly, the larger Zn^{2+} ions with slower transport may result in lower permeability, while the smaller Ni^{2+} ions permeate faster. However, we found that Zn^{2+}, Cu^{2+}, and Ni^{2+} permeabilities at different concentrations were not correlated with the size of the ions (Fig. 7). The Zn^{2+} permeabilities ranked top and the Ni^{2+} was the slowest species. Therefore, the ion transfer rate might be mainly attributed to the ion affinity with the D2EHPA carrier (Fig. 1). A particular carrier exhibits pH-dependent extraction behavior towards different cations [60]. According to the literature [61,62], the D2EHPA extraction rate favors Zn^{2+} under acidic condition (pH around 2). When the pH was increased to 4 or higher, Cu^{2+} could be extracted at 90%, whereas Ni^{2+} was extractable in a pH>6 solution. As the feed solution was at pH 2, it is expected that the D2EHPA mostly favors Zn^{2+} ion transport and least favors Ni^{2+}. Our results are in agreement with this prediction, although the permeability for Zn^{2+} and Cu^{2+} is not significantly different in this work.

Another finding about single ion permeability is that the permeability at 2 mM resulted in the highest permeability values for these three ions (Fig. 7) among the tested concentrations. One would expect that higher feed concentration may facilitate dissolution and complex formation in the isopar-L phase. Here this is not the case. We speculate that overdosing ion concentration may increase viscosity in the feed and membrane phases, resulting in higher mass-transfer resistance and lower diffusivity and permeability. Besides, the limited amount of the carrier (0.4 M D2EHPA) became more inadequate for the higher ion concentration (20 mM), leading to lower ion permeability at this concentration. A similar behavior of the ion transport decrease at overdosing ion concentrations due to the saturation of the membrane phase also is reported in the literature [63-65].

4. Ion Permeability from Binary Solutions

Fig. 8(a) shows the Zn^{2+} concentration increase with time from

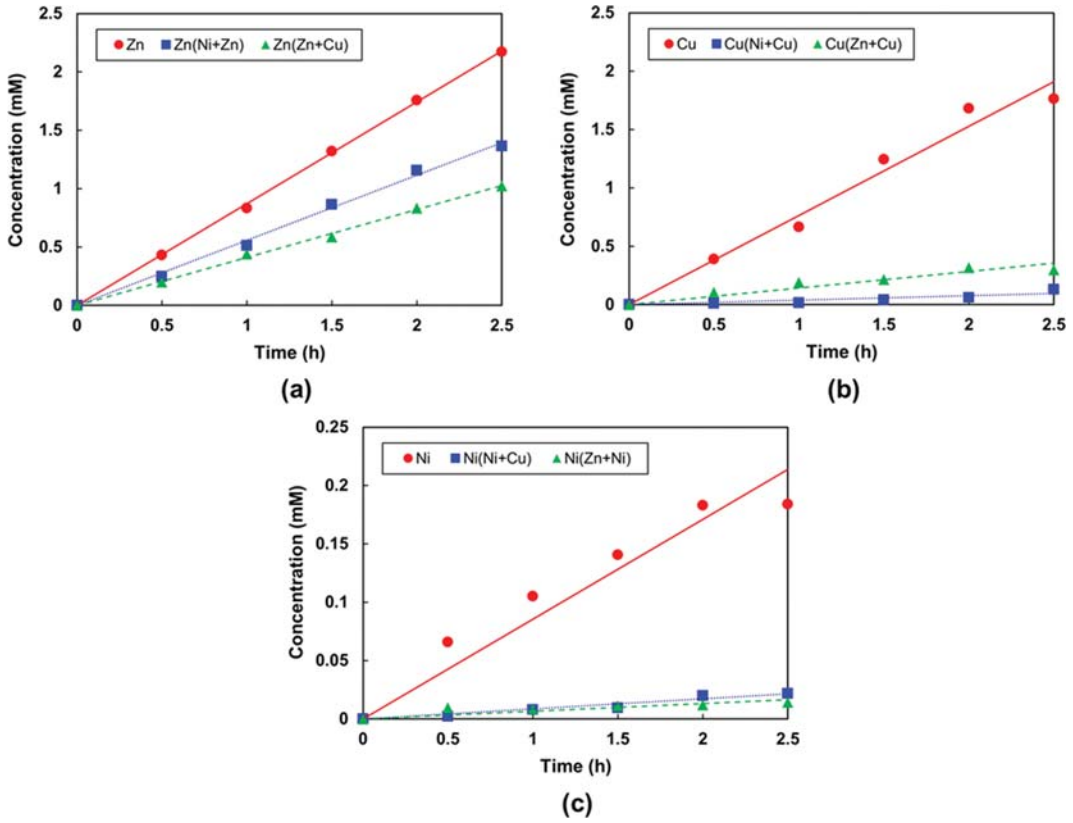

Fig. 8. Permeated ion concentrations of single and binary (a) Zn^{2+}, (b) Cu^{2+}, and (c) Ni^{2+} ions through SLM from 20 mM solutions (with 1.8 M of initial H_2SO_4 concentration in strip solution and 0.4 M D2EHPA in isopar-L for membrane phase).

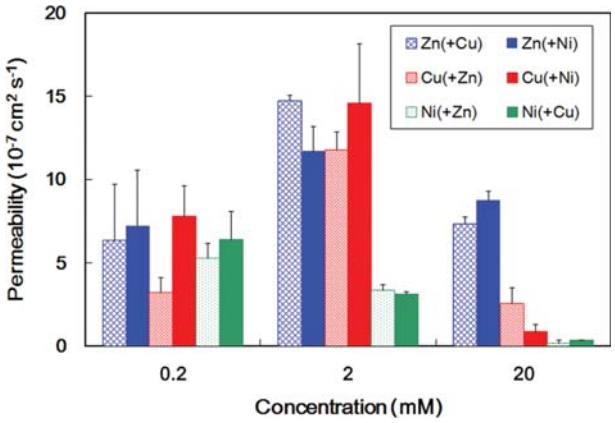

Fig. 9. Permeabilities of Zn^{2+}, Cu^{2+}, and Ni^{2+} from binary solutions of various concentrations (with 1.8 M of initial H_2SO_4 concentration in strip solution and 0.4 M D2EHPA in isopar-L for membrane phase). Error bars indicate 95% confidence intervals.

binary salt solutions, along with that from $ZnSO_4$ single solution for comparison. Compared with the Zn^{2+} permeability (P_{Zn}) of 9.83±0.57×10^{-7} cm^2 s^{-1} from the single solution (as shown in the previous section), the presence of co-ions of Ni^{2+} or Cu^{2+} decreased the Zn^{2+} permeability. When Ni^{2+} was present in the feed solution, the Zn^{2+} ions permeated at a slower rate, resulting in an average permeability $P_{Zn(+Ni)}$ of 8.73±0.81×10^{-7} cm^2 s^{-1} (Fig. 9). With the presence of Cu^{2+} co-ion, the Zn^{2+} ions permeated at an even slower rate, with a permeability $P_{Zn(+Cu)}$ of 7.35±0.36×10^{-6} cm^2 s^{-1} (Fig. 9).

The Cu^{2+} concentration increased with time from the binary solutions, as shown in Fig. 8(b). The permeability of single Cu^{2+} ions, P_{Cu}, was determined as 9.01±2.33×10^{-7} cm^2 s^{-1} (previous section). When Zn^{2+} was present in the feed solution, the Cu^{2+} ions permeated at a significant reduced rate and the average permeability $P_{Cu(+Zn)}$ was calculated to be 2.56±0.95×10^{-7} cm^2 s^{-1} (Fig. 9). With the presence of Ni^{2+} co-ion, the Cu^{2+} ions permeated at an even slower rate, resulting in a permeability $P_{Cu(+Ni)}$ of 0.89±0.08×10^{-7} cm^2 s^{-1} (Fig. 9).

As shown in the previous section, single Ni^{2+} ions transported with a permeability of 1.17±0.20 cm^2 s^{-1}. When Zn^{2+} or Cu^{2+} was present in the Ni^{2+} solution, the permeating Ni^{2+} ions from the binary solutions exhibited slower diffusion rates than the single solution (Fig. 8(c)). The average permeability of $P_{Ni(+Zn)}$ and $P_{Ni(+Cu)}$ was 0.15±0.06×10^{-7} cm^2 s^{-1} and 0.35±0.01×10^{-6} cm^2 s^{-1}, respectively (Fig. 9).

An interference effect of the second metal was also observed in another work [58]. Simultaneous transport of mixed feed with various mass ratios (Cd:Pb) showed both the extraction and recovery were less than those of pure metals. This tendency is explained by the presence of a higher proportion of one metal decreasing the amount of available driving force (concentration difference) for transport of the other metal in a binary mixture. Another possible explanation is that the competition between the two metals to form complexes with the fixed amount of the carrier (0.4 M D2EHPA) reduced permeability rates of both the metals.

The ion permeabilities from less concentrated binary solutions (0.2 and 2 mM) are summarized in Fig. 9. Again, the ion permeabilities were higher in the 2 mM solutions than those in the 0.2 and 20 mM. In the low concentration (0.2 mM), the ion permeabilities were in a similar range. In the medium concentration (2 mM), Ni^{2+} permeabilities were significantly lower than Zn^{2+} and Cu^{2+} ions. At 20 mM solution, the Zn^{2+} permeabilities were higher than those of Ni^{2+} and Cu^{2+} ions.

From the binary mixtures, the permeability ratios of co-existing ions can be used to calculate the actual selectivity (α_{binary}) in that particular ion pair, as shown in Table 1. The α_{binary} values from 0.2 and 2 mM solutions were not significantly different (1.22-4.63). As the feed concentration was increased to 20 mM, permeation between Zn^{2+} and Ni^{2+} became differentiable. The ions in the high concentration feed would compete for the limited amount of D2EHPA for complexation and diffusion. Zinc ions have strong affinity with D2EHPA at the low pH value and form complexes at a higher level than Ni^{2+}. Therefore the α_{binary} value for the Zn/Ni pair was significantly improved.

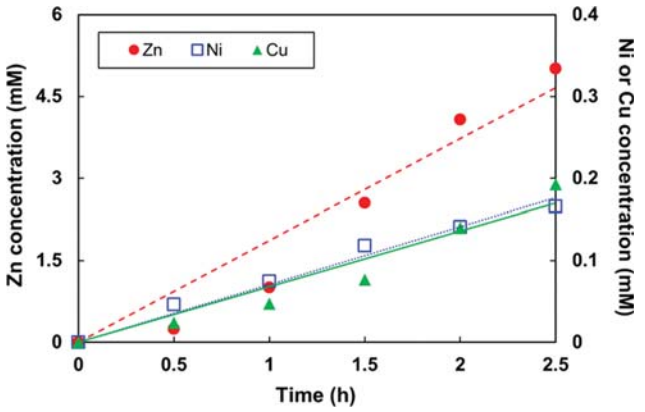

Fig. 10. Time resolved permeated Zn^{2+} (left axis), Ni^{2+} and Cu^{2+} (right axis) concentrations from 20 mM, ternary mixture of Zn^{2+}, Cu^{2+} and Ni^{2+} solutions (1.8 M of initial H_2SO_4 concentration in receiving solution and 0.4 M D2EHPA in isopar-L in membrane phase).

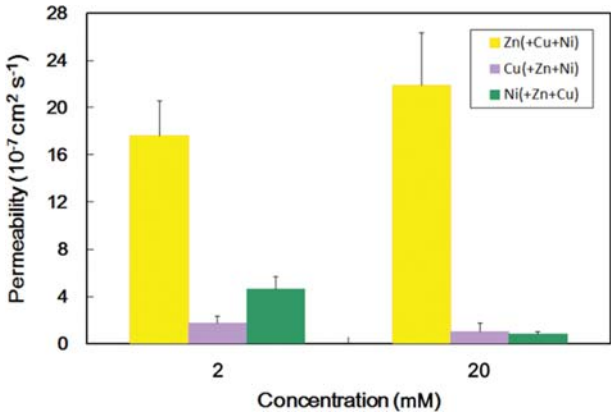

Fig. 11. Permeabilities of Zn^{2+}, Cu^{2+}, and Ni^{2+} from ternary solutions of 2 and 20 mM (with 1.8 M of initial H_2SO_4 concentration in strip solution and 0.4 M D2EHPA in isopar-L for membrane phase). Error bars indicate 95% confidence intervals.

Table 2. A comparison of ion permeation and selectivity rates of supported liquid membranes

Feed	SLM (Carrier/solvent/support)	Strip	Ion flux (J) or permeability (P)	Ion selectivity	Ref.
Zn^{2+} 0.88-6.82 mM, pH 2-3	D2EHPA 2.66 mM/kerosene/PVDF	H_2SO_4 1 M	J Zn^{2+}: 6×10^{-8}-1.15×10^{-6} mol m^{-2} s^{-1}	-	[69]
Zn^{2+} 100 ppm, pH 4	PC-88A 0.2 M/kerosene/Teflon	Distilled water (buffered pH 1.8)	J Zn^{2+}: 1.56×10^{-9} mol cm^{-2} s^{-1}	-	[48]
Cu^{2+} 50 ppm, pH 3.5	D2EHPA 30%/*n*-Decane/PP D2EHPA 30%/*n*-Decane/PES	H_2SO_4 (pH 1.6)	J Cu^{2+}: 28.7 mmol m^{-2} h^{-1} J Cu^{2+}: 39.7 mmol m^{-2} h^{-1}	-	[70]
Cu^{2+} 0.1-100 mM, pH 5.5	HPBI 0.01 M/$CHCl_3$/PP	HNO_3 0.1 M	J Cu^{2+}: $0.35\text{-}7.05\times10^{-5}$ mol m^{-2} s^{-1}	-	[47]
Ni^{2+} 255.58 mM, pH 6.37	D2EHPA 1.15 M/kerosene/PP	H_2SO_4 2.39%	J Ni^{2+}: 6.99×10^{-5} mol m^{-2} s^{-1}	-	[71]
Cu^{2+}, Ni^{2+}, Zn^{2+} or Mn^{2+} 50 ppm, pH 3.5	D2EHPA 50%/kerosene/PP	H_2SO_4 (pH 1.5)	J Cu^{2+}: 36.71 mmol m^{-2} h^{-1} J Ni^{2+}: 5.44 mmol m^{-2} h^{-1} J Zn^{2+}: 29.11 mmol m^{-2} h^{-1} J Mn^{2+}: 23.73 mmol m^{-2} h^{-1}	$Cu^{2+}>Zn^{2+}>Mn^{2+}>Ni^{2+}$[a]	[67]
Zn^{2+} 7.64 mM and Cu^{2+} 7.86 mM, pH 2.5	TOPS-99 0.1 M/kerosene/PP	H_2SO_4 0.9 M	J Zn^{2+}: 2.49×10^{-5} mol m^{-2} s^{-1} J Cu^{2+}: 4.01×10^{-8} mol m^{-2} s^{-1}	$Zn^{2+}>Cu^{2+}$	[32]
Cu^{2+} 100 ppm and Ni^{2+} 100 ppm, in ammoniacal solution 2 M	TRPO 10% and M5640 20% /kerosene/PVDF	H_2SO_4 50 g/L	J Cu^{2+}: 1.91×10^{-5} mol m^{-2} s^{-1} (>98.4% of Cu^{2+} and <6.1% of Ni^{2+} transferred)	$Cu^{2+}>Ni^{2+}$	[22]
Ni^{2+} 500 ppm and Mg^{2+} 100 ppm, pH 4.5	LIX 84-I 0.4 M and D2EHPA 0.4 M /kerosene/PP	H_2SO_4 1.5 M	P Ni^{2+}: 42.8×10^{-7} m s^{-1} P Mg^{2+}: 8.18×10^{-7} m s^{-1}	$Ni^{2+}>Mg^{2+}$	[23]
Ag^{+} 10 mM, Cu^{2+} 10 mM and Zn^{2+} 10 mM	[2.2.1] macrobicyclic polyethers 0.001 M/chloroform/PP	Double distilled water	J Ag^{+}: 2.46×10^{-10} mol cm^{-1} s^{-1} J Cu^{2+}: 4.49×10^{-10} mol cm^{-1} s^{-1} J Zn^{2+}: 3.78×10^{-10} mol cm^{-1} s^{-1}	$Cu^{2+}>Zn^{2+}>Ag^{+}$	[33]
Cu^{2+} 8.97 mM, Zn^{2+} 40.83 mM, Co^{2+} 27.49 mM, and Ni^{2+} 420.51 mM, pH 3.4-4.8	LIX 84I 20%/kerosene/PP	H_2SO_4 0.9 M	J Cu^{2+}: $1.528\text{-}2.629\times10^{-5}$ mol m^{-2} s^{-1} (Zn^{2+}, Co^{2+} and Ni^{2+} permeation: 0.076-0.187 mM)	$Cu^{2+}>Zn^{2+}>Co^{2+}>Ni^{2+}$	[72]
Zn^{2+} 40.75 mM, Co^{2+} 27.405 mM and Ni^{2+} 420.344 mM, pH 1.2-3.65	TOPS-99 0.1 M/kerosene/PP		J Zn^{2+}: $1.76\text{-}5.00\times10^{-5}$ mol m^{-2} s^{-1} (Co^{2+} and Ni^{2+} permeation: 0.017-0.118 mM and 0.0511-0.17 mM)	$Zn^{2+}>Co^{2+}>Ni^{2+}$	
Co^{2+} 27.219 mM and Ni^{2+} 420.02 mM, pH 5.0-6.8	Cyanex 272 0.6 mM/kerosene/PP		J Co^{2+}: $2.64\text{-}6.97\times10^{-5}$ mol m^{-2} s^{-1} (Ni^{2+} permeation: 0.34 mM)	$Co^{2+}>Ni^{2+}$	

Table 2. Continued

Feed	SLM (Carrier/solvent/support)	Strip	Ion flux (*J*) or permeability (*P*)	Ion selectivity	Ref.
Ca^{2+} 160 ppm, Cd^{2+} 25 ppm, Cu^{2+} 40 ppm, Pb^{2+} 40 ppm, Zn^{2+} 20 ppm and Ni^{2+} 40 ppm, pH 3.5	LIX-84 10%/kerosene /(alumina/silica/DCDMS membrane)	HNO_3 1% (pH 1)	*J* Cu^{2+}: 2.3×10^{-10} mol cm^{-2} s^{-1} Other metals: unmeasurable flux	$Cu^{2+}>Ca^{2+}$, Cd^{2+}, Pb^{2+}, Zn^{2+}, Ni^{2+}	[24]
Cu^{2+} 228 ppm, Cd^{2+} 14.578 ppm, Pb^{2+} 6.512 ppm, Ni^{2+} 2.902 ppm, Co^{2+} 1.396 ppm and Fe^{3+} 0.854 ppm, pH 3	D2EHPA 40%/kerosene/PE	HNO_3 2 M (pH 0.3)	*P* Cu^{2+}: 0.78×10^{-6} cm s^{-1} *P* Cd^{2+}: 7.0×10^{-6} cm s^{-1} *P* Pb^{2+}: 20.0×10^{-6} cm s^{-1} *P* Ni^{2+}: 0.53×10^{-6} cm s^{-1} *P* Co^{2+}: 6.0×10^{-6} cm s^{-1} *P* Fe^{3+}: 3.7×10^{-6} cm s^{-1}	$Pb^{2+}>Cd^{2+}>Co^{2+}>Fe^{3+}>Cu^{2+}\approx Ni^{2+}$	[68]
Zn^{2+}, Cu^{2+} or/and Ni^{2+} 0.2 mM, 2 mM or 20 mM, pH 2	D2EHPA 0.4 M/isopar-L/PP	H_2SO_4 1.8 M	*P* Zn^{2+}: $6.36\text{-}21.88\times10^{-7}$ cm^2 s^{-1} *P* Cu^{2+}: $0.89\text{-}11.8\times10^{-7}$ cm^2 s^{-1} *P* Ni^{2+}: $0.15\text{-}6.36\times10^{-7}$ cm^2 s^{-1}	$Zn^{2+}\geq Cu^{2+}>Ni^{2+a}$ $Zn^{2+}>Cu^{2+}$, $Cu^{2+}>Ni^{2+}$, $Zn^{2+}>Ni^{2+}$ $Zn^{2+}>Cu^{2+}\approx Ni^{2+}$	This study

[a]From single solutions

Di(2-ethylhexyl) phosphoric acid (D2EHPA); polyvinylidene fluoride (PVDF); 2-ethylhexylphosphoric acid mono-2-ethylhexyl ester (PC-88A); polypropylene (PP); polyethersulphone (PES); 3-phenyl-4-benzoylisoxazol-5-one (HPBI); di-2-ethyl hexyl phosphoric acid (TOPS-99); bis(2,4,4-trimethyl pentyl) phosphinic acid (Cyanex 272); trialkyphosphine oxide (TRPO); 2-hydroxy-5-nonylacetophenone oxime (LIX 84-I); dichlorodimethylsilane (DCDMS); polyethylene (PE); tri-octylphosphine oxide (TOPO)

5. Ion Permeabilities from Ternary Solutions

The ternary mixtures containing 20 mM of $ZnSO_4$, $CuSO_4$ and $NiSO_4$ were fed to the permeation cells and the ion permeation rates were determined. The transported Zn^{2+} concentration through the SLM increased to 5.00 mM after 2.5 h (as shown in Fig. 10). The permeability of Zn^{2+} was $21.88\pm4.46\times10^{-7}$ cm^2 s^{-1} through SLM (Fig. 11), which was higher than that from single and binary solutions. The permeated concentrations of Cu^{2+} and Ni^{2+} were 0.19 mM and 0.17 mM, respectively, at 2.5 h (Fig. 10). The permeability of Cu^{2+} and Ni^{2+} was $1.03\pm0.72\times10^{-7}$ cm^2 s^{-1} and $0.81\pm0.20\times10^{-7}$ cm^2 s^{-1}, respectively (Fig. 11). The Zn/Cu and Zn/Ni selectivity values from the ternary mixtures reached values of 21.2 and 27.0, respectively (Table 1).

The ternary mixtures containing 2 mM of $ZnSO_4$, $CuSO_4$ and $NiSO_4$ were also fed to the permeation cells and the ion permeation rates were determined. The permeability values of Zn^{2+}, Cu^{2+}, and Ni^{2+} were $17.58\pm2.97\times10^{-7}$ cm^2 s^{-1}, $1.73\pm0.59\times10^{-7}$ cm^2 s^{-1}, and $4.61\pm1.08\times10^{-7}$ cm^2 s^{-1}, respectively, as shown in Fig. 11.

Under acidic conditions, the D2EHPA tends to extract Zn^{2+} ions and inhibit Cu^{2+} and Ni^{2+} ions [61]. Conversely, D2EHPA favors extracting the Ni^{2+} ions under alkaline conditions [23,66]. It can be explained that the acidic environments in the donor phase (pH 2) and strip phase (H_2SO_4 1.8 M) greatly enhanced the transport of Zn^{2+} ions. This preferred transport toward Zn^{2+} is especially intensified in the ternary solutions and at high feed ionic concentrations (Table 1).

Fig. 11 summarizes the ion permeabilities from ternary solutions of 2 mM (equivalent to 6×10^{-5} mole for each ion) and 20 mM (6×10^{-4} mole for each ion). The Zn^{2+} permeability in the concentrated feed was improved and the Cu^{2+} and Ni^{2+} permeabilities were suppressed. As more favorable Zn^{2+} ions were present in the feed, the D2EHPA (equivalent to ~10^{-5} mole) would prefer the complex formation with Zn^{2+}, with little carrier available for Cu^{2+} and Ni^{2+}. Therefore, the Cu^{2+} and Ni^{2+} transports resembled those with D2EHPA-lean circumstances (Fig. 4), with permeability values approaching ca. 10^{-8} cm^2 s^{-1}.

Table 2 shows a summary comparison on various metal ion permeation and selectivity using SLMs. It can be observed that ion flux/permeability coefficients and selectivity orders varied according to composition and characteristics of the feeds, SLMs and strips. In the SLMs with D2EHPA carrier [67,68], Ni^{2+} permeated less than Zn^{2+} or Cu^{2+}, which was in agreement with this study's findings. However, the ion permeation rates of single solutions reported by Molinari et al. [67] displayed a slightly different order from that of the present study, i.e., $Cu^{2+}>Zn^{2+}$ vs. $Zn^{2+}\geq Cu^{2+}$. It might be related to its higher feed pH of 3.5, at which the D2EHPA favored more Cu^{2+} transport. This study demonstrated ion selectivity of several unities to several tens, consistent with most of the other works [22,23,33,67,68]. By working on various multi-ionic solutions (single, binary and ternary) of various ionic concentration (0.2 mM, 2 mM and 20 mM), the present study disclosed that extracting Zn^{2+} from Cu^{2+} and/or Ni^{2+} mixtures was most efficient from ternary ionic mixes of high concentrations. The SLM impregnated with D2EHPA in this study therefore has great potential for separating actual Zn-rich effluents, which are usually multi-component and/or highly concentrated systems.

CONCLUSIONS

The ionic permeabilities of Zn^{2+}, Cu^{2+}, and Ni^{2+} were measured through supported liquid membranes, consisting of D2EHPA in isopar-L solvent. Increasing the D2EHPA or H_2SO_4 strip solution concentration can improve the ion transport rates. Single, binary, and ternary mixtures of these salts were prepared at 0.2, 2, and 20 mM concentrations and the ionic permeability and selectivity (α) were measured. The ionic permeability was in the 10^{-7}-10^{-6} cm^2 s^{-1} range. From single solutions, Zn^{2+} and Cu^{2+} exhibited comparable permeability while Ni^{2+} was the least permeable ion. For binary mixtures, the low concentration (0.2 mM) solutions did not differentiate between the ions ($\alpha<2$). In 2 and 20 mM binary solutions, Zn^{2+} was the fastest permeating species and the selectivity of ion pairs was higher than those with 0.2 mM feed solutions. The selectivity was significantly improved in the ternary mixtures, without sacrificing the fast-permeating Zn^{2+} ion transport rate. Overall, the supported membrane containing D2EHPA is efficient for extracting Zn^{2+} from ionic mixtures.

ACKNOWLEDGEMENTS

The authors acknowledge the financial support from Chang Gung University grant number [BMRP326] and Chang Gung Memorial Hospital grant number [CMRPG2GO422 and CMRPD2F0053].

SUPPORTING INFORMATION

Additional information as noted in the text. This information is available via the Internet at http://www.springer.com/chemistry/journal/11814.

REFERENCES

1. N. K. Srivastava and C. B. Majumder, *J. Hazard. Mater.*, **151**, 1 (2008).
2. T.-Y. Yeh and H.-C. Chen, *Environ. Sci. Pollut. Res.*, **24**, 21517 (2017).
3. R. Prakorn, N. Kwanta and P. Ura, *Korean J. Chem. Eng.*, **21**, 1212 (2004).
4. F. Fu, L. Xie, B. Tang, Q. Wang and S. Jiang, *Chem. Eng. J.*, **189-190**, 283 (2012).
5. Q. Chang and G. Wang, *Chem. Eng. Sci.*, **62**, 4636 (2007).
6. X. Z. Yuan, Y. T. Meng, G. M. Zeng, Y. Y. Fang and J. G. Shi, *Colloids Surf., A: Physicochem. Eng. Aspects*, **317**, 256 (2008).
7. S. A. Nabi, R. Bushra and M. Shahadat, *J. Appl. Polym. Sci.*, **125**, 3438 (2012).
8. P. Otrembska and J. Gega, *Sep. Sci. Technol. (Philadelphia)*, **47**, 1345 (2012).
9. R.-S. Juang and R.-C. Shiau, *J. Membr. Sci.*, **165**, 159 (2000).
10. Z. V. P. Murthy and L. B. Chaudhari, *J. Hazard. Mater.*, **160**, 70 (2008).
11. B. Mukherjee and A. K. Mitra, World Water and Environmental Resources Congress 2003, Philadelphia, Pennsylvania, United States, 1229 (2003).
12. K. Noel Jacob, S. Senthil Kumar, A. Thanigaivelan, M. Tarun and D. Mohan, *J. Mater. Sci.*, **49**, 114 (2014).

13. M. Monier, D. M. Ayad and A. A. Sarhan, *J. Hazard. Mater.*, **176**, 348 (2010).
14. Z. Cheng, A. L. K. Tan, Y. Tao, D. Shan, K. E. Ting and X. J. Yin, *Int. J. Photoenergy*, **2012**, 5 (2012).
15. G. Hota, B. R. Kumar, W. J. Ng and S. Ramakrishna, *J. Mater. Sci.*, **43**, 212 (2008).
16. P. Zaheri, H. Abolghasemi, T. Mohammadi and M. G. Maraghe, *Korean J. Chem. Eng.*, **32**, 1642 (2015).
17. T. A. Kurniawan, G. Y. S. Chan, W.-H. Lo and S. Babel, *Chem. Eng. J.*, **118**, 83 (2006).
18. H. K. Haghighi, M. Irannajad and D. Moradkhani, *Korean J. Chem. Eng.*, **35**, 53 (2018).
19. P. K. Parhi, *J. Chem.*, **2013**, 11 (2013).
20. N. L. Mai, S. H. Kim, S. H. Ha, H. S. Shin and Y.-M. Koo, *Korean J. Chem. Eng.*, **30**, 1804 (2013).
21. X. Yang, A. Fane and K. Soldenhoff, *Ind. Eng. Chem. Res.*, **42**, 392 (2003).
22. H. Duan, S. Wang, X. Yang, X. Yuan, Q. Zhang, Z. Huang and H. Guo, *Chem. Eng. Res. Design*, **117**, 460 (2017).
23. I. Van De Voorde, L. Pinoy and R. F. De Ketelaere, *J. Membr. Sci.*, **234**, 11 (2004).
24. C. A. Cooper, Y. S. Lin and M. Gonzalez, *J. Membr. Sci.*, **229**, 11 (2004).
25. A. J. B. Kemperman, D. Bargeman, T. Van Den Boomgaard and H. Strathmann, *Sep. Sci. Technol.*, **31**, 2733 (1996).
26. W. Ho and T. K. Poddar, *Environ. Prog. Sustainable Energy*, **20**, 44 (2001).
27. E. Bringas, M. F. San Román and I. Ortiz, *J. Chem. Technol. Biotechnol.*, **81**, 1829 (2006).
28. R. H. Crabtree, *Chem. Rev.*, **85**, 245 (1985).
29. R. N. R. Sulaiman and N. Othman, *J. Environ. Chem. Eng.*, **6**, 1814 (2018).
30. A. Gherrou, H. Kerdjoudj, R. Molinari and E. Drioli, *Sep. Purif. Technol.*, **28**, 235 (2002).
31. S. B. Kunungo and R. Mohapatra, *J. Membr. Sci.*, **105**, 227 (1995).
32. K. Sarangi and R. P. Das, *Hydrometallurgy*, **71**, 335 (2004).
33. O. Arous, A. Gherrou and H. Kerdjoudj, *Desalination*, **161**, 295 (2004).
34. P. Venkateswaran, A. N. Gopalakrishnan and K. Palanivelu, *J. Environ. Sci.*, **19**, 1446 (2007).
35. W. Zhang, C. Cui and Z. Hao, *Chinese J. Chem. Eng.*, **18**, 48 (2010).
36. A. W. Lothongkum, Y. Khemglad, N. Usomboon and U. Pancharoen, *J. Alloys Compd.*, **476**, 940 (2009).
37. C. Li, F. Xie, Y. Ma, T. Cai, H. Li, Z. Huang and G. Yuan, *J. Hazard. Mater.*, **178**, 823 (2010).
38. M. B. Mansur, *Rem: Revista Escola de Minas*, **64**, 51 (2011).
39. F. Fu and Q. Wang, *J. Environ. Manage.*, **92**, 407 (2011).
40. C. Onac, A. Kaya, D. Ataman, N. A. Gunduz and H. K. Alpoguz, *Chinese J. Chem. Eng.*, **27**, 85 (2019).
41. A. Gössi, W. Riedl and B. Schuur, *J. Chem. Technol. Biotechnol.*, **93**, 629 (2018).
42. L. J. Lozano, C. Godínez, A. P. de los Ríos, F. J. Hernández-Fernández, S. Sánchez-Segado and F. J. Alguacil, *J. Membr. Sci.*, **376**, 1 (2011).
43. P. Zaheri, T. Mohammadi, H. Abolghasemi and M. Ghannadi Maraghe, *Chem. Eng. Res. Design*, **100**, 81 (2015).
44. M. Shamsipur, F. Falaki and F. J. D. Shemirani, *Desalin. Water Treat.*, **57**, 25705 (2016).
45. L. D. Nghiem, P. Mornane, I. D. Potter, J. M. Perera, R. W. Cattrall and S. D. Kolev, *J. Membr. Sci.*, **281**, 7 (2006).
46. S. J. Lue, H. J. Juang and S. Y. Hou, *Sep. Sci. Technol.*, **37**, 463 (2002).
47. L. Mitiche, S. Tingry, P. Seta and A. Sahmoune, *J. Membr. Sci.*, **325**, 605 (2008).
48. A. M. Tarditi, J. Marchese and M. E. Campderrós, *Desalination*, **228**, 226 (2008).
49. B.-Y. Wang, C. K. Tseng, C.-M. Shih, Y.-L. Pai, H.-P. Kuo and S. J. Lue, *J. Membr. Sci.*, **464**, 43 (2014).
50. P. Deblay, M. Minier and H. Renon, *Biotechnol. Bioeng.*, **35**, 123 (1990).
51. A. M. St John, S. P. Best, Y. Wang, M. J. Tobin, L. Puskar, R. Siegele, R. W. Cattrall and S. D. Kolev, *Aust. J. Chem.*, **64**, 930 (2011).
52. M. Resina, J. Macanás, J. de Gyves and M. Muñoz, *J. Membr. Sci.*, **289**, 150 (2007).
53. F. Zhang, J. Dai, A. Wang and W. Wu, *Inorg. Chim. Acta*, **466**, 333 (2017).
54. J. He, Y. Li, X. Xue, H. Ru, X. Huang and H. Yang, *RSC Adv.*, **5**, 74961 (2015).
55. H. Nadimi, A. Amirjani, D. H. Fatmehsari, S. Froozi, and A. Azadmehr, *Miner. Eng.*, **69**, 177 (2014).
56. A. Sürücü, V. Eyüpoglu and O. Tutkun, *Desalination*, **250**, 1155 (2010).
57. D. D. Pereira, S. D. F. Rocha and M. B. Mansur, *Sep. Purif. Technol.*, **53**, 89 (2007).
58. K. K. Bhatluri, M. S. Manna, P. Saha and A. K. Ghoshal, *J. Membr. Sci.*, **459**, 256 (2014).
59. E. R. Nightingale, *J. Phys. Chem.*, **63**, 1381 (1959).
60. L. Gotfryd and G. Pietek, *Physicochem. Probl. Miner. Process.*, **49**, 133 (2013).
61. C. Group, MCT Redbook: Solvent Extraction Reagents and Applications, Cognis Group, U.S.A. (2007).
62. C. Y. Cheng, *Hydrometallurgy*, **56**, 369 (2000).
63. G. Nikam, K. Mahanwar, S. Sabale and B. Mohite, *Sep. Sci. Technol.*, **48**, 493 (2013).
64. G. Nikam and B. Mohite, *Res. J. Chem. Sci.*, **2**, 75 (2012).
65. A. A. Mohammed and M. A. Hussein, *Association of Arab Universities J. of Engineering Sciences*, **25**, 65 (2018).
66. P. M. Cole and K. C. Sole, *Miner. Process. Extr. Metall. Rev.*, **24**, 91 (2003).
67. R. Molinari, T. Poerio and P. Argurio, *J. Membr. Sci.*, **280**, 470 (2006).
68. N.-E. Belkhouche, M. A. Didi, R. Romero, J. Å. Jönsson and D. Villemin, *J. Membr. Sci.*, **284**, 398 (2006).
69. T.-C. Huang and R.-S. Juang, *J. Membr. Sci.*, **31**, 209 (1987).
70. R. Molinari, P. Argurio and T. Poerio, *Sep. Purif. Technol.*, **70**, 166 (2009).
71. P. Parhi, K. Sarangi and S. J. M. Mohanty, *Min., Metall. Explor.*, **29**, 225 (2012).
72. P. K. Parhi and K. Sarangi, *Sep. Purif. Technol.*, **59**, 169 (2008).

Supporting Information

Competition of mixed divalent ions through supported liquid membranes: Co-ion and concentration effects on permeability

Thi Tuong Van Tran[*,], Chiao-Chen Hsu[*], Selvaraj Rajesh Kumar[*], and Shingjiang Jessie Lue[*,***,****,*****,†]**

*Department of Chemical and Materials Engineering and Green Technology Research Center, Chang Gung University, Guishan District, Taoyuan 333, Taiwan
**Institute of Environmental Science, Engineering and Management, Industrial University of Ho Chi Minh City, Go Vap District, Ho Chi Minh City, Vietnam
***Department of Radiation Oncology, Chang Gung Memorial Hospital, Guishan District, Taoyuan 333, Taiwan
****Department of Safety, Health and Environmental Engineering, Ming-Chi University of Technology, Taishan District, New Taipei City 243, Taiwan
*****R&D Center for Membrane Technology, Chung Yuan Christian University, Chung Li District, Taoyuan 320, Taiwan
(*Received 14 February 2019 • accepted 1 June 2019*)

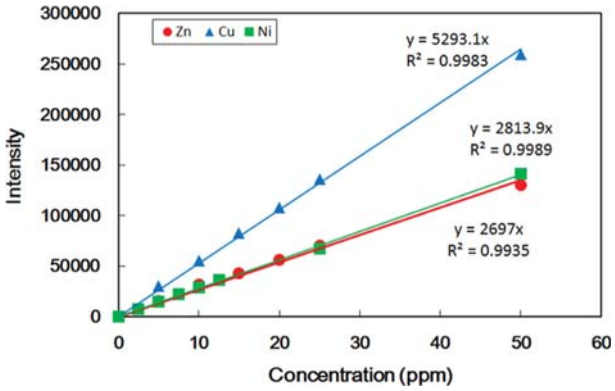

Fig. S1. Calibration curves of Zn^{2+}, Cu^{2+}, and Ni^{2+} using ICP-OES.